Thermal conduction in $Al_xGa_{1-x}N$ alloys and thin films

Weili Liu and Alexander A. Balandin[a)]
Nano-Device Laboratory,[b)] Department of Electrical Engineering, University of California–Riverside, Riverside, California 92521

(Received 8 November 2004; accepted 19 January 2005; published online 25 March 2005)

We report on experimental and theoretical investigation of thermal conduction in $Al_xGa_{1-x}N$ alloys. A focus of this study is on understanding the effect of the Al mass fraction x and temperature on thermal conductivity in $Al_xGa_{1-x}N$ thin films. The thermal conductivity of a set of $Al_xGa_{1-x}N$ thin films as well as a pure GaN sample was measured using the differential 3ω technique in the temperature range from 80 to 400 K. Application of the virtual-crystal model allowed us to elucidate the strength of the mass-difference and strain-field-difference phonon scattering in $Al_xGa_{1-x}N$ alloy system. The obtained thermal-conductivity temperature dependence indicates the high degree of disorder in the system. The measured variation of the thermal conductivity with the Al fraction x is in good agreement with the theory predictions. The measured data and calculation procedure are useful for evaluating the self-heating effect in $Al_xGa_{1-x}N$/GaN heterostructure field-effect transistors and for the device structure optimization. © *2005 American Institute of Physics*. [DOI: 10.1063/1.1868876]

I. INTRODUCTION

GaN and GaN-based III-V alloy semiconductors are promising materials for the next generation of high-power electronic, microwave, and optoelectronic devices.[1–3] One of the important issues in further development of GaN high-power technology is self-heating.[3–6] Self-heating in GaN-based field-effect transistors (FETs) can result in an abrupt increase of the local temperature[5,6] and lead to the drain-source current reduction, current gain dispersion, current collapse, and, possible, to a thermal-induced breakdown at voltage levels lower than theoretical predicted value.[7] Thus, it is important to know the accurate values of thermal conductivity in GaN thin films and $Al_xGa_{1-x}N$ alloys used in fabrication of $Al_xGa_{1-x}N$/GaN heterostructure field-effect transistors (HFETs). The role of the alloy scattering on thermal conduction and the thermal-conductivity dependence on temperature in $Al_xGa_{1-x}N$ films also need to be determined for accurate modeling of GaN FET performance.

Several groups have reported investigation of the thermal conductivity in GaN films.[8–10] The previous theoretical studies of the thermal conductivity of bulk GaN, conducted by Zou and co-workers[11,12] on the basis of the Callaway–Klemens approach, have demonstrated that impurities and dislocations can significantly reduce the thermal conductivity of GaN films. There have been indications that the thermal boundary resistance at the interface between GaN and substrate materials is much larger than the predictions of the acoustic mismatch model.[13] A much less investigated problem is thermal conduction in $Al_xGa_{1-x}N$ alloy system. $Al_xGa_{1-x}N$ alloys are used as the barrier layer in GaN-based HFETs. High-Al content barriers were proposed for increasing the sheet carrier density in the device channel[14,15] and for flicker noise suppression in $Al_xGa_{1-x}N$/GaN HFETs.[16] In conventional technologically important alloy systems, such as Si_xGe_{1-x} and $Al_xGa_{1-x}As$, the variation of thermal conductivity with the mass fraction x has been systematically investigated in every detail.[17–19] Despite their practical importance, no such studies have been reported for $Al_xGa_{1-x}N$ alloy system.

In this paper we report on experimental and theoretical investigations of the dependence of the thermal conductivity of $Al_xGa_{1-x}N$ alloys and on Al mass fraction x. The paper also provides experimental details pertinent to our recent letter,[20] which described a rather unusual temperature dependence of the thermal conductivity in $Al_xGa_{1-x}N$ thin films. Our calculations are based on the virtual-crystal model while experimental results are obtained using the differential 3ω technique. The rest of the paper is organized as follows. In Sec. II, we describe the virtual-crystal model and introduce $Al_xGa_{1-x}N$ specific parameters such as atomic weight, atomic volume, Debye temperature, and relevant phonon-scattering terms. Section III presents details of the experimental measurements of $Al_xGa_{1-x}N$ thin films and GaN reference sample, as well as comparison of the experimental and modeling results. We give our conclusions in Sec. IV.

II. THE VIRTUAL-CRYSTAL MODEL FOR AlGaN ALLOYS

In this section we recast the virtual crystal model for $Al_xGa_{1-x}N$. Originally this approach has been used for Si_xGe_{1-x} and $(Ga,In)_xAs_{1-x}$ alloys. In semiconductor crystals, heat is mostly carried by acoustic phonons. According to the measurements by Florescu *et al.*,[21] in GaN with doping concentration around 10^{16}–10^{18} cm^{-3}, the electronic contribution to thermal conductivity is about 1000 times smaller than that of phonons. Thus, in this study we limit ourselves to the lattice, i.e., phonon, thermal conduction.[22] Within this model, the alloys are assumed to be a random mixture of

[a)]Author to whom correspondence should be addressed; electronic mail: alexb@ee.ucr.edu
[b)]Web-site address: http://ndl.ee.ucr.edu/

atoms, with different masses and elemental volumes, arranged in a specific lattice. The basic idea of the virtual-crystal model is to replace the disordered lattice by the ordered virtual crystal with randomly distributed atoms of constituent materials. The acoustic phonons are scattered by the disorder perturbations and the anharmonicity of the virtual crystal. Following this idea, we transform the disordered $Al_xGa_{1-x}N$ alloy into the ordered virtual crystal with the virtual atomic weight, atomic volume, and lattice constants.

The virtual atomic weight M is assumed to be the mass average of different components of the alloy. For the $Al_xGa_{1-x}N$ alloy, M can be written as

$$M = xM_{\mathrm{AlN}} + (1-x)M_{\mathrm{GaN}}, \tag{1}$$

where x is the mass fraction of AlN component in the alloy, and M_{AlN} and M_{GaN} are the mean atomic weights of AlN and GaN components in the alloy, respectively. The virtual atomic volume is given by Vegard's law through the equation

$$\delta = x\delta_{\mathrm{AlN}} + (1-x)\delta_{\mathrm{GaN}}. \tag{2}$$

Here δ, the characteristic length scale of the lattice, is defined as the cubic root of the virtual atomic volume. The characteristic length scales δ_{AlN} and δ_{GaN} of AlN and GaN, respectively, are consequently defined as the cubic roots of the mean atomic volumes of AlN and GaN components in the alloy. The elastic constant c_{ik} is proportional to q^2/δ^4,[23] where q is the electronic charge. Keyes[24] obtained the following correlation formula:

$$c_{ik}\delta^4 \approx \text{const.} \tag{3}$$

This formula is, in general, applicable to the group IV and III-V crystals. From this formula and from the known elastic constants and atomic volume of either GaN or AlN, and Eq. (2), one can obtain the elastic constants c_{ik} of the virtual crystal. Once c_{ik} are obtained, the acoustic-phonon velocity can be determined by the elastic dynamics. For the wurtzite-structure AlGaN alloy, we can write the following expressions for the longitudinal v_L and transverse $v_{T1}(v_{T2})$ sound velocities:

$$\begin{aligned} v_L &= \sqrt{c_{11}/\rho_{\mathrm{AlGaN}}}, \\ v_{T1} &= \sqrt{c_{44}/\rho_{\mathrm{AlGaN}}}, \\ v_{T2} &= \sqrt{(c_{11}-c_{12})/2\rho_{\mathrm{AlGaN}}}. \end{aligned} \tag{4}$$

The nonuniformity of the Brillouin zone and corresponding differences in the phonon velocities and cutoff frequencies among longitudinal and transverse branches cause the discrepancy in various models.[25] Assuming that the experimentally measured Debye frequency is the average cutoff frequency of all three acoustic branches, the corresponding average phonon group velocity can be written as

$$v = \frac{3}{v_{T1}^{-1} + v_{T2}^{-1} + v_L^{-1}}. \tag{5}$$

The Debye temperature Θ of the virtual crystal can be calculated from the elastic constants. As derived in Ref. 26, $\Theta \propto (\delta c_{ik}/M)^{1/2}$, combining this expression with Eq. (3) leads to the following result:

$$\Theta M^{1/2}\delta^{3/2} = \alpha, \tag{6}$$

where α is a parameter independent of temperature T. In our calculations, we assume α to be a constant determined from that of material parameters of GaN and AlN. The value of α is then used to calculate the Debye temperature of the virtual crystal. The Gruneisen anharmonicity constant γ is given by

$$\gamma = -\frac{d\ln\Theta}{d\ln\delta^3}. \tag{7}$$

Combining Eqs. (6) and (7), we obtain for our case the value $\gamma = 0.5$.

The phonon thermal conductivity in Callaway's approximation can be written as[27]

$$k_{\mathrm{ph}} = \frac{\kappa}{2\pi^2 v}\left(\frac{\kappa T}{\hbar}\right)^3 \int_0^{\Theta/T} \frac{x^4 e^x}{(e^x-1)^2}\tau_c\left(1+\frac{\beta}{\tau_N}\right)dx, \tag{8}$$

where κ and $\hbar$ are the Boltzmann constant and Planck constant, respectively, while $\tau_c^{-1} = \tau_R^{-1} + \tau_N^{-1}$ is the combined relaxation time, obtained by Matthiessen summation of the resistive relaxation τ_R and normal scattering relaxation τ_N times. Parameter β is defined by the standard expression,

$$\beta = \int_0^{\Theta/T} \frac{x^4 e^x}{(e^x-1)^2}\frac{\tau_c}{\tau_N}dx \Bigg/ \int_0^{\Theta/T} \frac{x^4 e^x}{(e^x-1)^2}\left(1-\frac{\tau_c}{\tau_N}\right)\frac{1}{\tau_N}dx. \tag{9}$$

In the disordered $Al_xGa_{1-x}N$ bulk alloys and thin films, the point-defect phonon-scattering rate is expected to be very high, and one can safely assume that $\tau_c \ll \tau_N$ and $\tau_c \approx \tau_R$. Therefore, the thermal conductivity can be calculated using the simplified equation,

$$k_{\mathrm{ph}} = \frac{\kappa}{2\pi^2 v_s}\left(\frac{\kappa T}{\hbar}\right)^3 \int_0^{\Theta/T} \frac{x^4 e^x}{(e^x-1)^2}\tau_R dx, \tag{10}$$

where $\tau_R^{-1} = \tau_P^{-1} + \tau_U^{-1} + \tau_B^{-1}$, and τ_P, τ_U, and τ_B are the acoustic-phonon relaxation times on point defects, in umklapp processes, and in rough boundary scattering, respectively.

In the virtual-crystal model, the acoustic-phonon scattering by both impurities and alloy components can be categorized as the point-defect scattering. The point-defect scattering relaxation time, calculated by Klemens[28] from the perturbation theory, is

$$\tau_P^{-1} = \frac{\delta^3 \Gamma \omega^4}{4\pi v^3}, \tag{11}$$

where $\Gamma = \Gamma_{\mathrm{imp}} + \Gamma_{\mathrm{alloy}}$ is the point-defect scattering factor, and Γ_{imp} and Γ_{alloy} characterize the contributions from the impurities and alloy disorder, respectively. Γ_{imp} depends on the doping density and the growth method. From the data reported in the literature[29,30] we extract the values of Γ_{imp} equal to 1.3×10^{-4} and 3.2×10^{-4} for GaN and AlN, respectively. For $Al_xGa_{1-x}N$ alloys, Γ_{imp} value may vary for different samples. However, it is much smaller than Γ_{alloy} when $x \neq 0$ or 1. Here we adopt a component weighted Γ_{imp} for the $Al_xGa_{1-x}N$ alloys and thin films,

TABLE I. Material constants and parameters of GaN and AlN used in the model.

	GaN	AlN
Mean atomic weight (amu)	Ga: 69.72, Al: 26.98, N: 14.0.	
Mean atomic volume (cm^2/mol)	Ga: 11.8, Al: 10.0, N: 17.3.	
Debye temperature (K)	600	1150
Density (g/cm^3)	6.15	3.266
Elastic constants (Gpa)[a]	c_{11}: 390	c_{11}: 410
	c_{12}: 145	c_{12}: 149
	c_{44}: 105	c_{44}: 125
Lattice constants (Å)	a_0: 3.189	a_0: 3.122
	c_0: 5.186	c_0: 4.982

[a]The elastic constants of the virtual crystal can be calculated from either those of GaN or AlN using Eq. (3) described in the text.

$$\Gamma_{\text{imp}} = x_{\text{AlN}} 1.3 \times 10^{-4} + (1 - x_{\text{AlN}}) 3.2 \times 10^{-4}. \tag{12}$$

The Γ_{alloy} parameter can be written as

$$\Gamma_{\text{alloy}} = \sum_i x_i \left[[(M_i - M)/M]^2 + \varepsilon [(\delta_i - \delta)/\delta]^2 \right], \tag{13}$$

where i is the index for components GaN or AlN. The first term in the brackets is the mass-difference-induced scattering factor and the second term is the one caused by the strain-field difference. Conventionally, ε is considered as a phenomenological parameter specific for given materials system. We assume its value to be $\varepsilon = 39$, similar to Si_xGe_{1-x} alloy. A posterior check by comparison with the results of our measurements attests that it is a valid assumption. The umklapp scattering relaxation time in the high-temperature limit can be written as [31]

$$\tau_U^{-1} = \frac{\hbar \gamma^2 T \omega^2}{M v^2 \Theta} \exp\left(-\frac{\Theta}{3T} \right). \tag{14}$$

The boundary-scattering relaxation time is given in the Casimir limit as $\tau_N^{-1} = v/L$, where L is the dimension of the sample. In our simulations we use $L = 22$ mm. This value is estimated by fitting the peak position of our measured temperature-dependent thermal conductivity of AlN bulk crystal. Material properties, such as the atomic weights and atomic volumes of Ga, Al, and N atoms, are taken from the Mendeleev's periodic table. Other parameters for wurtzite GaN and AlN crystals are taken from Ref. 32. The parameters and constants used in the calculations are summarized in Table I.

We have validated the virtual-crystal model for $Al_xGa_{1-x}N$ alloys by first calculating the thermal conductivities of pure GaN and AlN crystals and comparing them with known experimental values. Figures 1(a) and 1(b) show the calculated thermal conductivity of AlN and GaN crystals, respectively. The results are presented for a wide temperature range. For comparison, we also indicated experimental data points from Refs. 29 and 30. One can see a good agreement in the absolute values and in the temperature dependence between the measured and calculated curves for AlN material. The agreement is also good for GaN for temperatures above 100 K. The discrepancy for GaN at the low-temperature limit, around the thermal-conductivity maximum, is explained by the simplicity of the boundary-scattering term, which does not take into account the exact shape of the sample or the surface quality. In the high-temperature region, where the boundary scattering plays a minor role, our calculations capture correctly the bulk phonon-scattering effects and predict the room temperature and the high-temperature thermal conductivity of GaN and AlN crystals very well. In this work we are more interested in thermal conduction in $Al_xGa_{1-x}N$ alloys at the room temperature and above since that is the operation regime for GaN FETs.

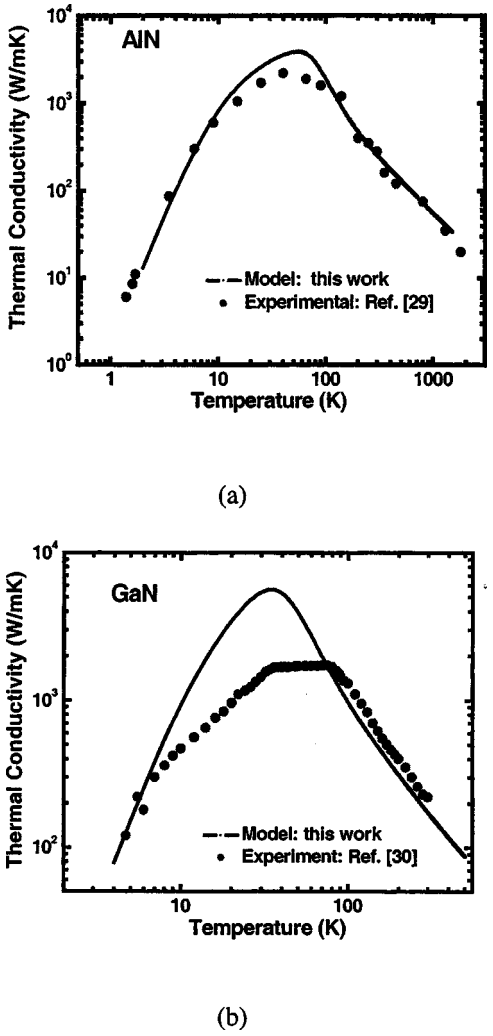

FIG. 1. Comparisons of the simulated thermal conductivities with the experimental data for (a) AlN and (b) GaN bulk crystals.

Figure 2 shows the simulated thermal conductivity as a function of temperature for the $Al_xGa_{1-x}N$ alloy with different Al mass fraction $x = 0.0$, 0.1, 0.5, 0.9, and 1.0. A strong reduction of the thermal conductivity due to the alloy scattering, i.e., the mass and strain-field-difference scatterings, is clearly seen in the figure. The reduction is observed over a wide temperature range from about 10 K all the way to 800 K. The thermal conductivity is more sensitive to the variation of the Al fraction at temperatures higher than 200 K, where the point-defect and phonon-phonon scatterings are dominant phonon relaxation processes. It can also be seen that the strongest reduction of the thermal conductivity happens

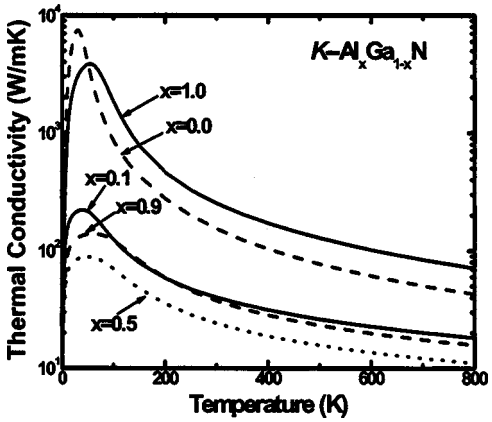

FIG. 2. Simulated thermal conductivity as a function of temperature for $Al_xGa_{1-x}N$ alloys with $x=1.0$, 0.9, 0.5, 0.1, and 0.0.

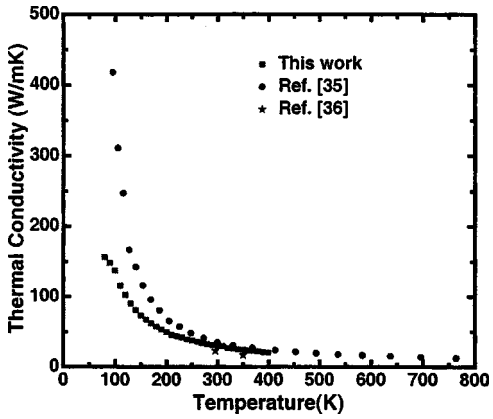

FIG. 3. Measured thermal conductivity of the sapphire (Al_2O_3) substrate as a function of temperature (solid squares). For comparison, the data points reported in Refs. 35 (solid circles) and 36 (stars) are also indicated.

when the Al or Ga mass fraction changes from 1.0 to 0.9. It indicates that a small portion of alien atoms in host material produces profound effect on the phonon scattering. Further addition of the alien atoms does not make such a big difference.

To completely validate the thermal-conductivity model and chose materials parameters for $Al_xGa_{1-x}N$ alloys, it is required to carry out comparison with experimental results. In Sec. III we report on measurements of the thermal conductivity in a set of $Al_xGa_{1-x}N$ films with different x values and a crystalline GaN sample. The measurements were carried out over the wide temperature range from 80 to 400 K using the 3ω technique.[33] Section III describes the experimental procedure and comparison of the experimental and modeling results.

III. MEASUREMENT OF THERMAL CONDUCTIVITY IN AlGaN ALLOYS

All investigated samples were grown on *c*-plane sapphire substrate by the modified hydride vapor-phase epitaxy (HVPE) technology.[34] Five samples investigated in this study are 18.5 -μm-thick pure GaN sample, 0.3-μm-thick $Ga_{0.09}Al_{0.91}N$, 0.6-μm-thick $Ga_{0.23}Al_{0.77}N$, 0.5-μm-thick $Ga_{0.33}Al_{0.67}N$, and 0.7-μm-thick $Al_{0.4}Ga_{0.6}N$ alloy thin films. The Al mass fraction of the alloy films was inspected with x-ray diffraction. The pure GaN sample was coated with a 93-nm-thick SiO_2 layer by the plasma-enhanced chemical-vapor deposition (PECVD) to provide electrical insulation required for the 3ω measurements. A Si reference sample, similarly coated with PECVD SiO_2 layer, was prepared for data subtraction in the differential 3ω technique. The thickness of the SiO_2 layer was measured by the Gaertner L116B Ellipsometer. The $Al_xGa_{1-x}N$ alloy samples were semi-insulating and no additional insulation layer was required.

On each sample, a 5-μm-wide 3ω heater thermometer composed of Cr (100 Å)/Au (1200 Å) was patterned by the photolithography, followed by the *e*-beam deposition and acetone lift-off. The 3ω measurements were conducted inside a Janis ST-300 vacuum cryostat using the home-built experimental setup in the temperature range from 80 to 400 K. A lock-in amplifier was used to provide the first harmonic input power and collect the third harmonic temperature rise signals from the sample. A numerical program based on the analytical solution of the 3ω heat conduction model for a layered medium was developed to fit the experimental data and obtain the thermal conductivity. The fitting procedure for the frequency-dependent temperature rise is described elsewhere.[20] To check the accuracy of the data reduction method, we also compared the measured thermal conductivity of sapphire substrate with the values obtained by other researchers. Figure 3 compares the thermal conductivity of the sapphire substrate measured in this work with the values reported by other groups.[35,36] The comparison shows that the *K* values of the sapphire substrate and its temperature dependence obtained in this work are in good agreement with the reported values. Some discrepancy at low temperature is attributed to the differences in the structure of the samples, examined by different groups. The variations in the temperature measurement techniques used by the two groups might also contribute to the discrepancy at low temperature. One should also take into account that, according to Ref. 36, the sapphire thermal conductivity of $c_{\|}$ direction (25 W/mK at 299 K) is slightly higher than that of $c_{\perp}$ direction (23 W/mK at 296 K). In our study, we neglect the small directional anisotropy and report the value averaged over the two directions. From this and several other test runs, the reliability of our experimental system is verified.

The measured thermal conductivity of all alloy films and GaN reference sample is shown in Fig. 4. The measured room-temperature thermal conductivity of the examined GaN film is 125 W/mK, which is very close to the values reported by both Lou *et al.*[8] and Florescu *et al.*[9] on lateral epitaxy overgrowth (LEO) GaN film although smaller than the bulk value reported by Slack *et al.*[37] The measured temperature dependence of the thermal conductivity in GaN film is typical for bulk crystals. The latter suggests that the bulk scattering processes, such as three-phonon umklapp and point-defect scattering, are the dominant phonon relaxation mechanisms in the sample. Some discrepancy in values obtained by different research groups is explained by variations in the material growth methods and sample quality. The extracted temperature dependence of the thermal conductivity

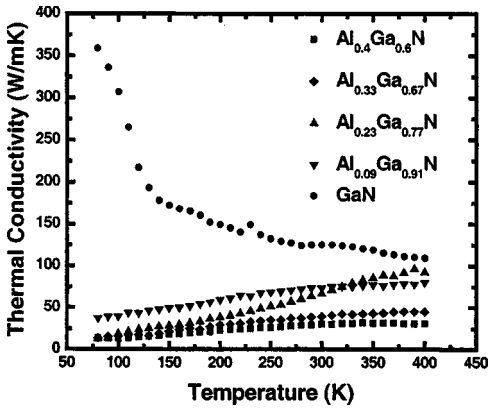

FIG. 4. Measured thermal conductivities of HVPE GaN, $Al_{0.09}Ga_{0.91}N$, $Al_{0.23}Ga_{0.77}N$, $Al_{0.33}Ga_{0.67}N$, and $Al_{0.4}Ga_{0.6}N$ thin films in the temperature range from 80 to 400 K.

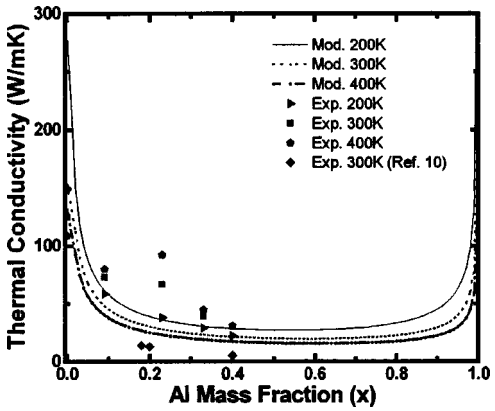

FIG. 5. Thermal conductivity as a function of the Al mass fraction x for $Al_xGa_{1-x}N$ alloy system at 200, 300, and 400 K. The theoretical curves are calculated from the virtual-crystal model, the points indicate the measured data. For comparison, the data points from Ref. 10 are also shown.

for GaN is $K \propto T^{-0.67}$. Its deviation from the $1/T$ rule is explained by the strong contribution of the point-defect scattering.[11,12]

The measured thermal conductivities of the $Al_xGa_{1-x}N$ alloy films are much smaller than that of GaN film. A noticeable feature observed in our measurements was that the thermal conductivity of the alloy films increases with temperature in the investigated temperature range. Such temperature dependence is normally observed in amorphous or completely disordered systems.[38] The measured dependence is similar to the one obtained for the polycrystalline AlGaN films[39] using the calculations based on the phonon-hopping transport model of Braginsky *et al.*[40] The observed thermal-conductivity reduction at low temperature can be attributed to the boundary or interface scattering, which is important at the submicron phonon transport regime.[41] As the thickness of the $Al_xGa_{1-x}N$ alloy samples is much smaller than that of the GaN reference sample, the boundary-scattering effect is expected to be relatively strong at low temperature. Figure 4 also shows that the thermal conductivity of the alloy system generally decreases with the increasing Al content from 0.0 to 0.4. The strongest reduction of the thermal conductivity in the wide temperature range from 80 to 300 K happens when the Al mass fraction changes from 0.0 to 0.09. This is in agreement with our modeling results described in Sec. II, which indicates that a small portion of Al atoms in the GaN host material produces profound effect on the phonon scattering.

In Fig. 5 we show the thermal conductivity in the $Al_xGa_{1-x}N$ alloy system as a function of the Al mass fraction x at 200, 300, and 400 K. The theoretical curves are obtained from the virtual-crystal model described in Sec. II and the data points are the measured results for the five samples. The data points, reported by Daly *et al.*[10] for 300 K, are also included in the figure for the direct comparison. It can be seen that the measured thermal-conductivity values, except those from the $Al_{0.23}Ga_{0.77}N$ thin film, are in reasonably good agreement with the theoretical predictions in both the absolute values and the trend of dependence on the Al mass fraction. The thermal-conductivity variation with the Al mass fraction, as demonstrated in both the theoretical curves and experimental data, shows a characteristic abrupt reduction when x increases from 0.0 to about 0.1, followed by a graduate approaches to minimum. The minimum thermal conductivity is achieved approximately at $x=0.6$. For the Al fraction larger than 0.9, the thermal conductivity starts to increase rapidly, approaching the bulk AlN crystal value. A similar trend was also observed in measurements reported in Ref. 10, although the absolute K values in that work were generally smaller than those obtained in this study. Overall the behavior is similar to that observed by Stohr and Klemm[19] for the undoped Si_xGe_{1-x} alloy system. The differences are related to the absolute values and the position of the minimum.

IV. SUMMARY

We have investigated the thermal conductivity of the $Al_xGa_{1-x}N$ alloy films both experimentally and theoretically. The thermal conductivity of a set of $Al_xGa_{1-x}N$ thin films as well as a pure GaN sample was measured using the differential 3ω technique in the temperature range from 80 to 400 K. The calculations of the thermal conductivity in $Al_xGa_{1-x}N$ alloy thin films were performed using the virtual-crystal model. The measured variation of the thermal conductivity with the Al fraction x is in good agreement with the theory predictions. The measured thermal-conductivity temperature dependence indicates the high degree of disorder in the system. The room-temperature thermal conductivity varies in the range from 25 to 55 W/mK when the Al mass fraction changes from 0.4 to 0.1. The strongest variation of the thermal conductivity is observed when the Al fraction changes in the range from 0.0 to 0.1 or from 0.9 to 1.0. The measured data and calculation procedure can be used for evaluating the self-heating effect in $Al_xGa_{1-x}N$/GaN heterostructure field-effect transistors and for the device structure optimization.

ACKNOWLEDGMENTS

This work was supported by the ONR Young Investigator Award (A.A.B.) and the National Science Foundation Early Faculty Development CAREER Award (A.A.B.).

[1]A. Balandin, S. V. Morozov, S. Cai, R. Li, K. L. Wang, G. Wijeratne, and C. R. Viswanathan, IEEE Trans. Microwave Theory Tech. **47**, 1413 (1999).
[2]M. E. Levinshtein, S. L. Rumyantsev, R. Gaska, J. W. Yang, and M. S. Shur, Appl. Phys. Lett. **73**, 1089 (1998).
[3]V. O. Turin and A. A. Balandin, Electron. Lett. **40**, 81 (2004).
[4]Y. Wu, B. P. Keller, S. Keller, J. J. Xu, B. J. Thibeault, S. P. Denbaars, and U. K. Mishra, IEICE Trans. Electron. **E82-C**, 1895 (1999).
[5]S. Nuttinck, R. Mukhopadhyay, C. Loper, S. Singhal, M. Harris, and J. Laskar, presented at European Microwave Week 2004, Amsterdam, The Netherlands, 2004 (Unpublished).
[6]M. Kuball, S. Rajasingam, A. Sarua, M. J. Uren, T. Martin, B. T. Hughes, K. P. Hilton, and R. S. Balmer, Appl. Phys. Lett. **82**, 124 (2003).
[7]L. F. Eastman *et al.*, IEEE Trans. Electron Devices **48**, 479 (2001); R. Gaska, A. Osinsky, J. W. Yang, and M. S. Shur, IEEE Electron Device Lett. **19**, 89 (1998).
[8]C.-Y. Lou, H. Marchand, D. R. Clarke, and S. P. Denbaars, Appl. Phys. Lett. **75**, 4151 (1999).
[9]D. I. Florescu, V. M. Asnin, F. H. Pollak, A. M. Jones, J. C. Ramer, M. J. Schurman, and I. Ferguson, Appl. Phys. Lett. **77**, 1464 (2000).
[10]B. C. Daly, H. J. Maris, A. V. Numikko, M. Kuball, and J. Han, J. Appl. Phys. **92**, 3820 (2002).
[11]D. Kotchetkov, J. Zou, A. A. Balandin, D. I. Florescu, and F. H. Pollak, Appl. Phys. Lett. **79**, 4316 (2001).
[12]J. Zou, D. Kotchetkov, A. A. Balandin, D. I. Florescu, and F. H. Pollak, J. Appl. Phys. **92**, 2534 (2002).
[13]T. A. Eckhause, Ö. Süzer, Ç. Kurdak, F. Yun, and H. Morkoç, Appl. Phys. Lett. **82**, 3035 (2003); K. A. Filippov and A. A. Balandin, MRS Internet J. Nitride Semicond. Res. **8**, 4 (2003).
[14]O. Ambacher *et al.*, J. Appl. Phys. **85**, 3222 (1999).
[15]J. P. Ibbetson, P. T. Fini, K. D. Ness, S. P. DenBaars, J. S. Speck, and U. K. Mishra, Appl. Phys. Lett. **77**, 250 (2000).
[16]A. Balandin , S. Morozov, G. Wijeratne, S. J. Cai, R. Li, J. Li, K. L. Wang, C. R. Viswanathan, and Y. Dubrovskii, Appl. Phys. Lett. **75**, 2064 (1999).
[17]B. Abeles, Phys. Rev. **131**, 1906 (1963).
[18]M. A. Afromowitz, J. Appl. Phys. **44**, 1292 (1973).
[19]H. Stohr and W. Klemm, Z. Anorg. Allg. Chem. **241**, 305 (1954).
[20]W. L. Liu and A. A. Balandin, Appl. Phys. Lett. **85**, 5230 (2004).
[21]D. I. Florescu, V. M. Asnin, F. H. Pollak, R. J. Molnar, and C. E. C. Wood, J. Appl. Phys. **88**, 3295 (2000).
[22]It should be pointed out that in the channel layer of the AlGaN/GaN HFET the local electronic thermal conductivity might be appreciable due to the formation of the high-density two-dimensional electron gas. This topic deserves a separate discussion and is reserved for future study.
[23]H. B. Huntington, in *Solid State Physics*, edited by F. Seitz and D. Turnbull (Academic, New York, 1958), Vol. 7.
[24]R. W. Keyes, J. Appl. Phys. **33**, 3371 (1962).
[25]M. G. Holland, Phys. Rev. **132**, 2461 (1963).
[26]E. F. Steigmeier, Appl. Phys. Lett. **3**, 6 (1963).
[27]J. Callaway, Phys. Rev. **113**, 1046 (1959).
[28]P. G. Klemens, Proc. Phys. Soc., London, Sect. A **68A**, 1113 (1955).
[29]G. A. Slack, R. A. Tanzilli, R. O. Pohl, and J. W. Vandersande, J. Phys. Chem. Solids **48**, 641 (1987).
[30]A. Jezowski, B. A. Danilchenko, M. Bockowski, I. Grzegory, S. Krukowski, T. Suski, and T. Paszkiewicz, Solid State Commun. **128**, 69 (2003).
[31]P. G. Klemens, in *Solid State Physics*, edited by F. Seitz and D. Turnbull, (Academic, New York, 1958), Vol. 7.
[32]V. Bougrov, M. E. Levinshtein, S. L. Rumyantsev, and A. Zubrilov, in *Properties of Advanced SemiconductorMaterials GaN, AlN, InN, BN, SiC, SiGe*, edited by M. E. Levinshtein, S. L. Rumyantsev, and M. S. Shur (Wiley, New York, 2001).
[33]D. G. Cahill, Rev. Sci. Instrum. **61**, 802 (1990).
[34]B. Lam *et al.*, Mater. Res. Soc. Symp. Proc. **639**, G6.4.1 (2001).
[35]The data is reported on the website http://users.mrl.uiuc.edu/cahill/tcdata/al2o3all.fin
[36]K. A. McCarthy and S. S. Ballard, J. Opt. Soc. Am. **41**, 1062 (1951).
[37]G. A. Slack, L. J. Schowalter, D. Morellic, and J. A. Freitas, Jr., J. Cryst. Growth **246**, 287 (2002).
[38]R. C. Zeller and R. O. Pohl, Phys. Rev. B **4**, 2029 (1971).
[39]D. Kotchetkov and A. A. Balandin, Mater. Res. Soc. Symp. Proc. **764**, C3.43 (2003).
[40]L. Braginsky, N. Lukzen, V. Shklover, and H. Hofmann, Phys. Rev. B **66**, 134203 (2002).
[41]A. Balandin, Phys. Low-Dim Structures 1/2, 1 (2000).